A role for Mints in transmitter release: Mint 1 knockout mice exhibit impaired GABAergic synaptic transmission

Angela Ho*, Wade Morishita†, Robert E. Hammer‡§, Robert C. Malenka†, and Thomas C. Südhof*†§¶‖

*Center for Basic Neuroscience, Departments of ¶Molecular Genetics and ‡Biochemistry, and §Howard Hughes Medical Institute, University of Texas Southwestern Medical Center, Dallas, TX 75390-9111; and †Department of Psychiatry and Behavioral Sciences, Nancy Friend Pritzker Laboratory, Stanford University School of Medicine, Stanford, CA 94304

Contributed by Thomas C. Südhof, December 19, 2002

Mints (also called X11-like proteins) are adaptor proteins composed of divergent N-terminal sequences that bind to synaptic proteins such as CASK (Mint 1 only) and Munc18-1 (Mints 1 and 2) and conserved C-terminal PTB- and PDZ-domains that bind to widely distributed proteins such as APP, presenilins, and Ca^{2+} channels (all Mints). We find that Mints 1 and 2 are similarly expressed in most neurons except for inhibitory interneurons that contain selectively high levels of Mint 1. Using knockout mice, we show that deletion of Mint 1 does not impair survival or alter the overall brain architecture, arguing against an essential developmental function of the Mint 1–CASK complex. In electrophysiological recordings in the hippocampus, we observed no changes in short- or long-term synaptic plasticity in excitatory synapses from Mint 1-deficient mice and detected no alterations in the ratio of α-amino-3-hydroxy-5-methyl-4-isoxazolepropionic acid (AMPA) to *N*-methyl-D-aspartate (NMDA) receptor-mediated synaptic currents. Thus the Mint 1–CASK complex is not required for AMPA- and NMDA-receptor functions or for synaptic plasticity in excitatory synapses. In inhibitory synapses, however, we uncovered an ≈3-fold increase in presynaptic paired-pulse depression, suggesting that deletion of Mint 1 impairs the regulation of γ-aminobutyric acid release. Our data indicate that Mints 1 and 2 perform redundant synaptic functions that become apparent in Mint 1-deficient mice in inhibitory interneurons because these neurons selectively express higher levels of Mint 1 than Mint 2.

Mints/X11-like proteins 1–3 are multidomain proteins composed of isoform-specific N-terminal sequences and common C-terminal PTB and PDZ domains (1–5). The divergent N-terminal sequences of Mints engage in isoform-specific interactions, whereas the shared C-terminal PTB and PDZ domains of all Mints participate in similar interactions. The N-terminal sequences of Mint 1 but not Mint 2 or 3 bind to CASK (6–8), a multidomain protein that in turn binds to cell-surface receptors (9–14). Furthermore, the N-terminal sequences of both Mints 1 and 2 but not Mint 3 bind to Munc18-1, a protein essential for synaptic vesicle exocytosis (2, 15). Conversely, the central PTB domains of all Mints bind to the cytoplasmic tail of APP (13, 16–18), whereas their PDZ domains bind to presenilins (5, 13), cell-surface receptors (11–14), Ca^{2+} channels (19), and the kinesin Kif17 (20). Thus Mints resemble adaptor proteins that connect distinct N-terminal interaction to similar C-terminal interactions. Despite the large number of known binding activities of Mints, their functions are still unclear.

In *Caenorhabditis elegans*, mutations in the Lin-10 gene [which encodes the only *C. elegans* Mint homolog (21)] cause two phenotypes: inhibition of vulva development (22) and neuronal abnormalities (23). The vulva phenotype is mediated by a protein complex formed by Lin-10 with two other gene products, Lin-2 (which encodes *C. elegans* CASK) and Lin-7 [a PDZ-domain protein, the vertebrate homologs of which are called Velis/Mals (6, 24)]. This complex is essential for the correct basolateral membrane localization of the epithelial growth factor receptor Let-23 in vulva precursor cells (22, 25). A similar protein complex is formed by the vertebrate homologs CASK, Velis/Mals, and Mint 1 (6, 8, 22, 24), suggesting that they may perform an evolutionarily conserved function. The second, neuronal phenotype caused by Lin-10 mutations in *C. elegans*, however, is independent of Lin-2–CASK and Lin-7–Velis, and correlates with mislocalization of α-amino-3-hydroxy-5-methyl-4-isoxazolepropionic acid (AMPA)-type glutamate receptors. This phenotype may be due to a general synaptic function of Lin-10–Mint that is independent of CASK (23).

In *C. elegans* (21) and vertebrate neurons (13), Mint 1–Lin-10 is concentrated at the Golgi apparatus but distributed throughout the axons and dendrites. A plausible explanation for the function of Lin-10 in *C. elegans* is that it directs the transport of proteins from the Golgi complex to their proper intracellular localization (21). This function may involve APP, which in mammalian neurons is colocalized with Mint 1 in the Golgi apparatus (13) and has been implicated in intracellular protein transport (26). Overexpression of Mints in transfected cells increases the steady-state levels of APP, alters β amyloid production, and impairs transcriptional activation of reporter genes by the cytoplasmic tail of APP, suggesting that Mints and APP interact *in vivo* (13, 27–29). Cotransfection of Munc18-1 potentiates the effects of Mint 1 consistent with a common action (30). However, in *C. elegans* decreased expression of the APP homolog apl-1 results in a phenotype that differs from that of Lin-10 mutants and thus cannot be explained by the interaction of Mint with APP (31). In the present study we tested the role of vertebrate Mint 1 in brain function using a knockout approach. Our data suggest that Mints 1 and 2 may perform redundant functions in synaptic transmission without an essential participation of the Mint 1–CASK complex.

NEUROSCIENCE

Methods

Generation and Characterization of Mint 1 Knockout Mice. Using genomic clones containing the 5′ end of the Mint 1 gene, we constructed a targeting vector for homologous recombination by standard procedures (32). In the targeting vector (designed to allow a conditional knockout of Mint 1), we flanked the large first coding exon of the Mint 1 gene (encoding residues 1–402) with loxP sites (to allow exon excision by cre recombinase), inserted into the 3′ intron a neomycin gene cassette (for positive selection after homologous recombination) surrounded by flp sites (to allow removal of the neomycin gene), and placed a diphtheria toxin gene next to the homologous sequence (for negative selection). Embryonic R1 stem cells (33) were electro-

Abbreviations: AMPA, α-amino-3-hydroxy-5-methyl-4-isoxazolepropionic acid; NMDA, *N*-methyl-D-aspartate; APV, 2-amino-5-phosphonovaleric acid; IPSC, inhibitory postsynaptic current; EPSC, excitatory postsynaptic current; LTP, long-term potentiation; GABA, γ-aminobutyric acid.

‖To whom correspondence should be addressed at: Center for Basic Neuroscience, University of Texas Southwestern Medical Center, 6000 Harry Hines Boulevard, NA4.118, Dallas, TX 75390-9111. E-mail: thomas.sudhof@utsouthwestern.edu.

porated with the Mint 1 targeting vector, and cell clones resistant to positive and negative selection were screened by Southern analysis to identify clones that resulted from a correct targeting event. Of 312 clones analyzed, 16 were targeted correctly, and 1 of these clones was used to generate mice containing the Mint 1 knockin. The floxed first exon was removed by cre-mediated recombination in the germ line (34). Genotyping was performed by PCR using oligonucleotide primers AH9914 vs. AH9916 (5′-CACTCAGCAATGGCGTCAAGC-3′ and 5′-CCACTCGCTATTGATCCCTGC-3′, respectively) for the wild-type allele (product size, 400 bp) and oligonucleotides AH9914 vs. AH0053 (5′-GGCGGACCGCTATCAGGACATAGCG-3′) for the mutant reaction (product size, 880 bp).

Protein Quantifications. Three adult littermate mice (≈2 months old) per genotype were killed, and brain tissue was isolated and homogenized in PBS/10 mM EDTA/1 mM PMSF. Brain proteins (40 μg per lane) were analyzed by SDS/PAGE and quantitative immunoblotting by using ^{125}I-labeled secondary antibodies and PhosphorImager (Molecular Dynamics) detection with GDP dissociation inhibitor, vasolin-containing protein, or annexin as internal standards (14, 32, 35).

Morphological Studies. Anesthetized adult mice (≈2 months old) were perfusion-fixed with 4% fresh paraformaldehyde and cryoprotected with 30% sucrose. Sections (30 μm) were permeabilized with 0.5% Triton X-100, blocked with 2% goat serum/0.1% Triton, and incubated with primary antibodies overnight at 4°C followed by incubation with horseradish peroxidase-coupled secondary antibodies. Sections were developed in 3,3′-diaminobenzidine tetrahydrochloride with nickel chloride as a metal enhancement and analyzed by standard light microscopy (32).

Electrophysiology. Transverse hippocampal slices (0.4 mm) were obtained from 4- to 8-week-old mice and allowed to recover in a holding chamber for at least 1.5 h before transfer to a recording chamber. Slices were maintained and perfused in external solution containing 119 mM NaCl, 2.5 mM KCl, 2 mM $MgSO_4$, 2.5 mM $CaCl_2$, 1 mM NaH_2PO_4, 26.2 mM $NaHCO_3$, 10 mM D-glucose, and 0.025–0.050 mM picrotoxin (saturated with 95% O_2/5% CO_2, pH 7.4). Extracellular field and whole-cell recordings were obtained in area CA1 basically as described (36). Inhibitory postsynaptic currents (IPSCs) were recorded in external solution containing 10 μM 2,3-dihydroxy-6-nitro-7-sulfamoylbenzo[*f*]-quinoxaline, 50 μM D-2-amino-5-phosphonovaleric acid (APV), and 5 μM (2*S*)-3-{[(1*S*)-1-(3,4-dichlorophenyl)ethyl]amino-2-hydroxypropyl}(phenylmethyl)phosphinic acid $GABA_B$ receptor antagonist (CGP 55845) without picrotoxin. IPSCs were evoked by a stimulating electrode placed at the border of stratum radiatum and stratum pyramidale. Frequency-dependent depression of excitatory postsynaptic currents (EPSCs) was elicited by a 14-Hz, 4-s train delivered to the Schaffer collaterals every 30 s. Posttetanic potentiation was induced by a 100-Hz, 0.5-s train in the presence of 0.1 mM D-APV. Long-term potentiation (LTP) was induced by four trains of 100-Hz stimuli lasting 1 s each separated by 20 s. AMPA- to *N*-methyl-D-aspartate (NMDA)-receptor ratios were obtained from cells voltage-clamped at +40 mV. The NMDA-receptor EPSC was determined by subtracting an averaged EPSC (15–50 responses) recorded in 0.1 mM D-APV (AMPA-receptor EPSC) from an averaged EPSC evoked in the absence of D-APV (AMPA-receptor + NMDA-receptor EPSC). Data were quantitated by measuring the amplitude of the EPSC and IPSC and the initial slope of the field excitatory postsynaptic potential.

Miscellaneous. SDS/PAGE and immunoblotting were performed with standard methods (37, 38) using the antibodies described (14, 35). All data shown are means ± SEMs. Statistical significance was determined by the Student's *t* test.

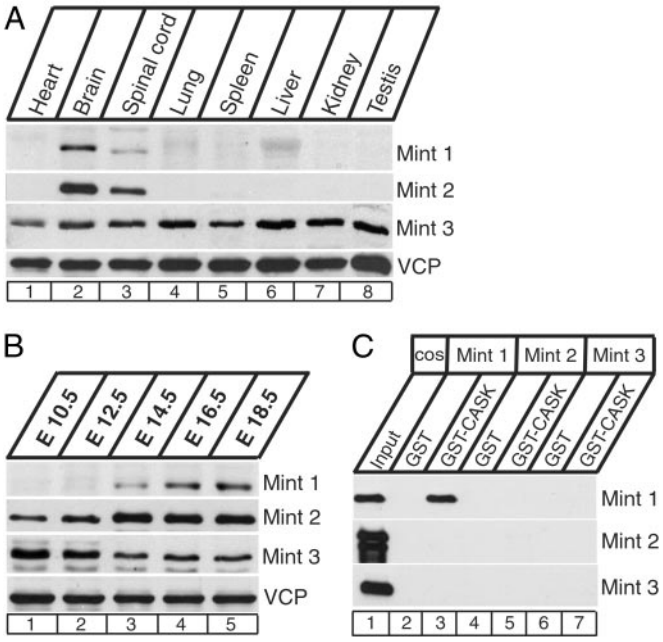

Fig. 1. Characterization of Mints. (*A*) Immunoblot analysis of mouse tissues for Mint 1–3 proteins. Vasolin-containing protein (VCP), a ubiquitously expressed protein, was used as a loading control. (*B*) Expression of Mints during embryonic development examined by immunoblotting of total mouse embryos at the indicated ages [embryonic days (E)10.5–18.5]. (*C*) Binding of Mints to CASK. Mints 1–3 were expressed in transfected COS cells and used for GST pull-down experiments with GST alone or GST–CASK. Bound proteins were analyzed with antibodies to the three Mints as indicated on the right.

Results

Properties and Expression of Mints. In preparation for a genetic analysis of Mint function, we examined the potential for redundancy among Mints. We first tested whether Mints are expressed in overlapping regional (Fig. 1*A*) and developmental (Fig. 1*B*) patterns. As observed (3, 39), we found that Mints 1 and 2 were detectable only in brain, but Mint 3 was ubiquitously expressed in all tissues tested (Fig. 1*A*). Immunoblotting of mouse embryos at different gestational stages showed that Mints 2 and 3 are synthesized at the earliest time point examined (embryonic day 10.5), whereas Mint 1 became only detectable 4 days later (Fig. 1*B*). The finding that Mint 1 is the last Mint isoform expressed is surprising, because Mint 1 is thought to be the only vertebrate homolog of Lin-10 (6, 8), which in turn performs an early developmental function in *C. elegans* (21). To ensure that Mint 1 is indeed the only Mint form that binds to CASK (and thus the only true Lin-10 homolog), we performed GST pull-down experiments in which binding of all Mints to CASK was tested (Fig. 1*C*). Only Mint 1 interacted with CASK, suggesting that Mint 1 exclusively participates in a tripartite complex with CASK and Velis analogous to the *C. elegans* Lin-2–Lin-7–Lin-10 complex (6).

Mint 1 Knockout Mice Are Viable and Fertile. We cloned the 5′ end of the murine Mint 1 gene, constructed a targeting vector, and produced mice with a mutant Mint 1 gene using standard homologous recombination in embryonic stem cells (Fig. 2*A*; ref. 33). The targeting procedure was designed to generate an inducible knockout by flanking the first coding exon of the Mint 1 gene with loxP sites and placing a neomycin resistance gene in the intron 3′ to the "floxed" exon. Mice containing the targeted

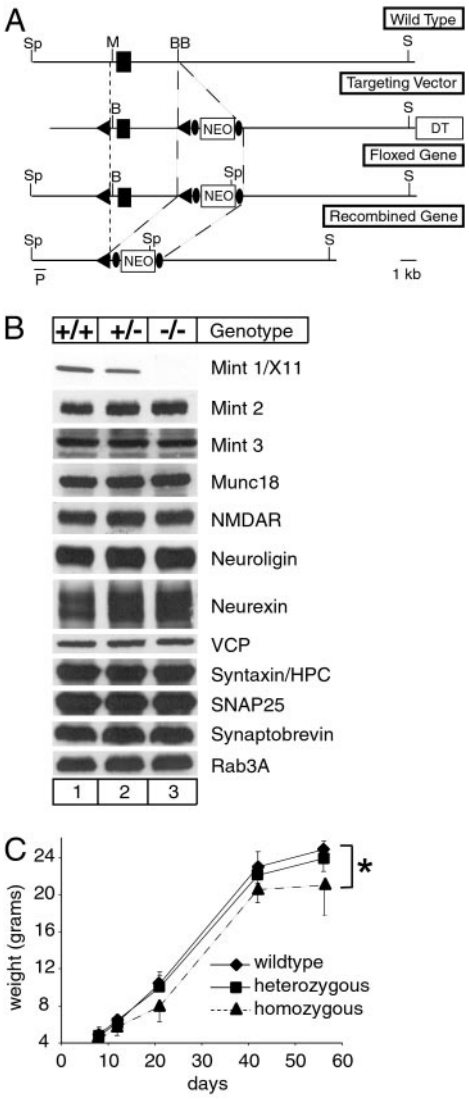

Fig. 2. Generation of Mint 1 knockout mice. (*A*) Homologous recombination strategy. Genomic clones of the Mint 1 gene containing the first coding exon (top diagram) were used to generate a targeting vector (second diagram from top), which was used for homologous recombination in embryonic stem cells (third diagram). In the targeting vector, the exon was flanked by loxP sites to allow conditional removal of the exon (bottom diagram), a neomycin resistance cassette (NEO) surrounded by flp recombination sites was inserted downstream, and a diphtheria toxin gene (DT) was attached for negative selection. (*B*) Immunoblot analysis of brain proteins from wild-type (+/+), heterozygous (+/−), and homozygous knockout (−/−) mice. Signals were visualized by enhanced chemiluminescence and quantified with ^{125}I-labeled secondary antibodies for a series of proteins (see Table 1). NMDAR, NMDA receptor; VCP, vasolin-containing protein. (*C*) Plot of the average weight (mean ± SEMs) of wild-type, heterozygous, and homozygous Mint 1 knockout mice as a function of age. The small decrease in the weight of the knockout mice is statistically significant ($n \geq 8$; $P < 0.05$, Student's t test).

floxed Mint 1 gene synthesized Mint 1 at approximately wild-type levels (data not shown). We then crossed the floxed mice to transgenic mice that express cre recombinase in the male germ line and generated knockout mice in which the floxed exon was deleted permanently (Fig. 2*A*).

Breeding of mutant mice revealed that homozygous knockout mice were viable and fertile, with a normal Mendelian ratio of genotypes in the offspring (80:161:96 for wild-type/heterozygous/homozygous mutant mice). Immunoblotting confirmed

Table 1. Quantitative levels of brain proteins in wild-type and Mint 1 mutant mice

Protein	Wild type	Heterozygous	Homozygous
Mint 1	100 ± 4	34 ± 3	5 ± 0
Mint 2	100 ± 15	106 ± 7	107 ± 7
Mint 3	100 ± 4	97 ± 9	90 ± 10
Munc18-1	100 ± 3	97 ± 2	94 ± 3
NMDA receptor	100 ± 3	97 ± 5	92 ± 8
Neuroligin 1	100 ± 9	111 ± 8	102 ± 9
Neurexins	100 ± 8	73 ± 2	94 ± 4
CASK	100 ± 7	112 ± 4	118 ± 9
Velis	100 ± 16	117 ± 12	109 ± 15
APP	100 ± 0	95 ± 6	98 ± 4
Syntaxin 1	100 ± 11	91 ± 4	90 ± 4
SNAP25	100 ± 12	92 ± 4	105 ± 7
Synaptobrevin 2	100 ± 3	111 ± 5	89 ± 4
Rab3a	100 ± 16	84 ± 3	84 ± 5

Proteins were measured in total brain homogenates by quantitative immunoblotting using ^{125}I-labeled secondary antibodies and PhosphorImager detection (32). The data shown are means ± SEMs from three independent determinations normalized for signals obtained with antibodies to vasolin-containing protein, GDP-dissociating inhibitor, and annexin as internal standards.

that the knockout mice lacked Mint 1 (Fig. 2*B*). Systematic weight measurements demonstrated a small but statistically significant decrease in size of the Mint 1 knockout mice, suggesting that the Mint 1 knockout mice are not completely normal (Fig. 2*C*).

To search for potential compensatory changes in Mint 1 knockout mice, we compared the expression of various proteins in wild-type and mutant mice but detected no significant changes (Fig. 2*B*; see Table 1). In particular, we observed no increases in Mints 2 and 3 or decreases in Munc18-1, CASK, and APP with which Mint 1 forms stoichiometric complexes (2, 6, 18). To rule out possible region-specific changes in protein levels, we investigated different brain areas but detected no obvious alterations in brain composition (Table 1 and data not shown). Because Mint 1 has been implicated as a possible regulator of APP cleavage (27–29) or of the transcriptional function executed by the APP cytoplasmic tail (13), we also examined APP. However, we found no difference between wild-type and knockout animals in the abundance of full-length APP or the C99/C83 breakdown products of APP (data not shown).

Brain Structure in Mint 1 Knockout Mice. Immunocytochemistry experiments demonstrated that deletion of Mint 1 did not cause major developmental brain abnormalities, for example in the layering of the cerebral cortex, formation of the cerebellum, or elaboration of the olfactory bulb (Figs. 3 and 4). In wild-type mice, Mint 1 was widely distributed in excitatory and inhibitory neurons throughout the brain, with highest levels in the olfactory glomeruli, the accessory olfactory bulb, and the medial habenulae (Fig. 3*A*). As expected, all Mint 1 staining was abolished in Mint 1 knockout mice. At the cellular level, Mint 1 was concentrated in neuronal cell bodies but present throughout the axons and dendrites. Immunostaining for the AMPA-type glutamate receptors GluR2 and GluR3 showed that their regional localization was not altered and confirmed that the overall structure of knockout and wild-type brains were indistinguishable (Fig. 3*B*).

Comparison of the staining patterns of Mints 1 and 2 in the hippocampus suggested that all excitatory and inhibitory neurons coexpressed Mints 1 and 2 (Fig. 4). However, interneurons that are probably inhibitory expressed Mint 1 at much higher levels than Mint 2. The specificity of staining was confirmed in

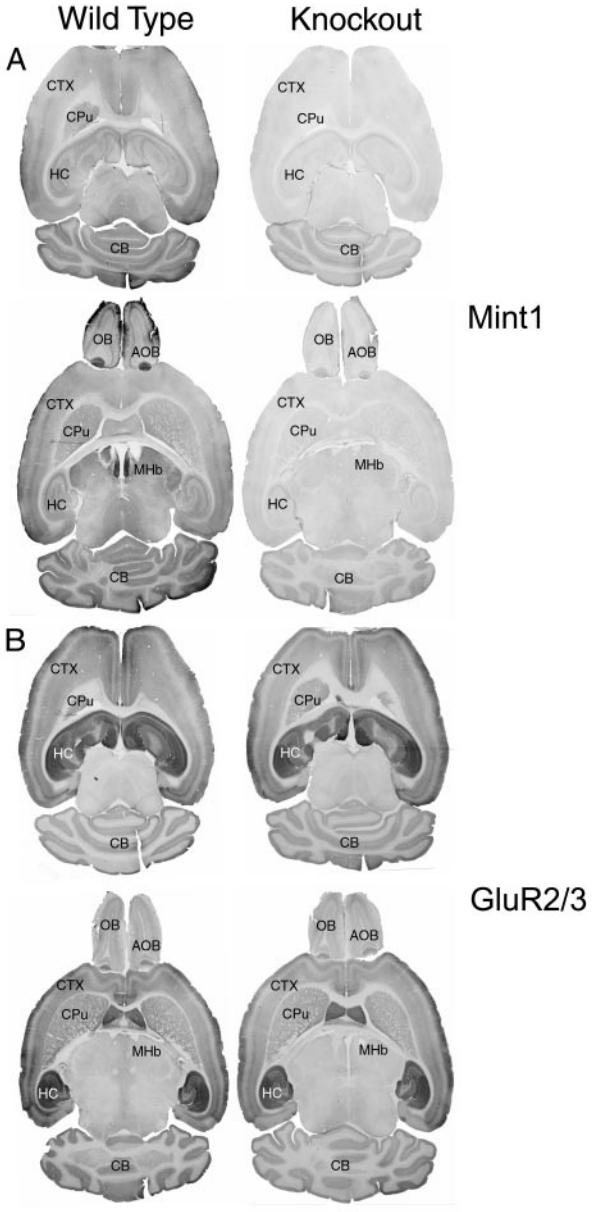

Fig. 3. Overall structure of wild-type (*Left*) and Mint 1 knockout (*Right*) brains viewed by immunocytochemistry with antibodies to Mint 1 (*A*) or GluR2/3 glutamate receptors (*B*). Brain sections were stained by using horseradish peroxidase-labeled secondary antibodies with metal-dependent signal enhancement as described (32). CTX, cerebral cortex; CPu, caudate putamen; HC, hippocampus; CB, cerebellum; OB, olfactory bulb; AOB, accessory OB; MHb, medial habenulae nuclei.

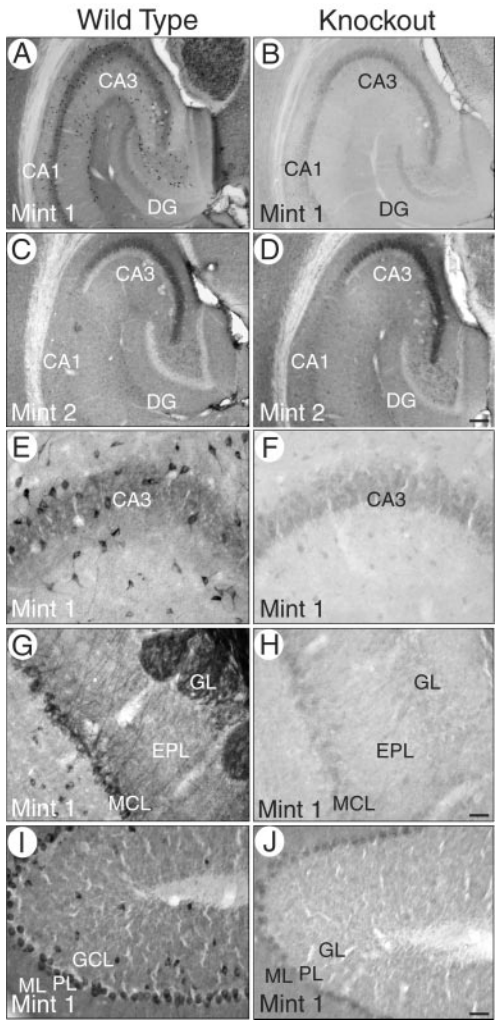

Fig. 4. Selective enrichment of Mint 1 in inhibitory interneurons. (*A–D*) Low-power views of the hippocampus from wild-type and Mint 1 knockout mice stained for Mint 1 (*A* and *B*) and Mint 2 (*C* and *D*) by using horseradish peroxidase-labeled secondary antibodies. (*E* and *F*) High-power views of the CA3 region of the hippocampus. (*G* and *H*) High-power views of the olfactory bulb. GL, glomerular layer; EPL, external plexiform layer; MCL, mitral cell layer. (*I* and *J*) Low-power views of the cerebellum from wild-type and Mint 1 knockout mice. ML, molecular layer; PCL, Purkinje cell layer; GCL, granule cell layer. (*E–J*) Stained for Mint 1. (Scale bars: *A–D*, *I*, and *J*, 100 μm; *E–H*, 30 μm.)

Mint 1 knockout mice in which all interneuron staining for Mint 1 was abolished, whereas the pattern of Mint 2 staining was unaltered (Fig. 4 *A–F*). In the olfactory bulb and cerebellum, Mint 1 was also present in all neurons and distributed throughout the neuropil but again was expressed at the highest levels in presumptive inhibitory neurons. Olfactory glomeruli that contain clusters of γ-aminobutyric acid (GABA)ergic interneurons were strongly stained, although excitatory mitral cells were also abundantly labeled, including the dendrites that contact the glomeruli (Fig. 4 *G* and *H*). In the cerebellum, interneurons in the granule cell layer and the inhibitory Purkinje cells were enriched in Mint 1, although the whole molecular layer (which primarily consists of excitatory granule cell axons and Purkinje cell dendrites) was also strongly labeled (Fig. 4 *I* and *J*). Apart from the lack of Mint 1 staining, no obvious abnormalities were observed in Mint 1 knockout mice in the shape and distribution of excitatory and inhibitory neurons.

Synaptic Function of Mint 1. Several observations have implicated Mint 1 in synaptic function (15, 19, 20, 23, 40). For example, Mints 1 and 2 bind strongly to Munc18-1 (2), which in turn is essential for Ca^{2+}-triggered synaptic vesicle exocytosis (15), and all Mints bind to Ca^{2+} channels, suggesting a possible role in presynaptic Ca^{2+} influx (19, 40). To test whether the Mint 1 knockout mice exhibit a synaptic phenotype, we used slice physiology and recorded excitatory and inhibitory synaptic responses in the CA1 region of the hippocampus (Figs. 5–7).

We first probed excitatory synaptic transmission in the CA1 region of the hippocampus. We compared the synaptic responses of wild-type and knockout mice in four paradigms that measure different types of short- and long-term synaptic plasticity: paired-pulse facilitation (Fig. 5*A*), use-dependent depression

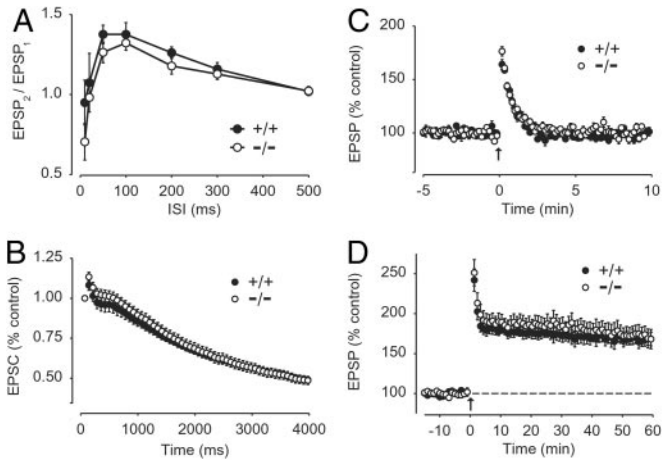

Fig. 5. Effect of Mint 1 deletion on excitatory synaptic transmission. Short- and long-term synaptic plasticity was examined in hippocampal slices from adult wild-type (+/+) and knockout (−/−) mice in the CA1 region. (*A*) Paired-pulse facilitation. Fibers were stimulated twice in close succession, and the relative size of the second compared with the first excitatory postsynaptic potential (EPSP) was monitored by field recordings at different interstimulus intervals (n = 5 slices from three wild-type and knockout mice). (*B*) Use-dependent depression of synaptic responses during repetitive stimulation. EPSCs were monitored by whole-cell voltage-clamp recordings in response to 14-Hz fiber stimulations and are normalized to the first response (n = 10 cells from three wild-type and knockout mice). (*C*) Posttetanic potentiation (PTP) elicited by a 100-Hz, 0.5-s stimulus train (arrow) in the presence of 0.1 mM D-APV. Synaptic responses were monitored by field recordings and are normalized to the initial response (n = 4 slices from two wild-type and 5 slices from two knockout mice). (*D*) LTP was elicited with four 100-Hz, 1-s stimulus trains with 20-s intervals between trains (arrow). Field excitatory postsynaptic potentials are normalized to baseline responses (n = 6 and 5 slices, respectively, from single wild-type and knockout mice). The data shown are means ± SEMs.

(Fig. 5*B*), posttetanic potentiation (Fig. 5*C*), and LTP (Fig. 5*D*). These measurements provide a sensitive, indirect assessment of fundamental properties of presynaptic neurotransmitter release and postsynaptic receptors. For example, alterations of release probability would result in changes in paired-pulse facilitation and posttetanic potentiation, inhibition of vesicle recycling would lead to enhanced use-dependent depression, and decreases in postsynaptic receptor function could interfere with LTP. In all these measurements, we observed no significant difference between wild-type and knockout mice, indicating that deletion of Mint 1 did not alter the fundamental properties of excitatory synaptic transmission (Fig. 5).

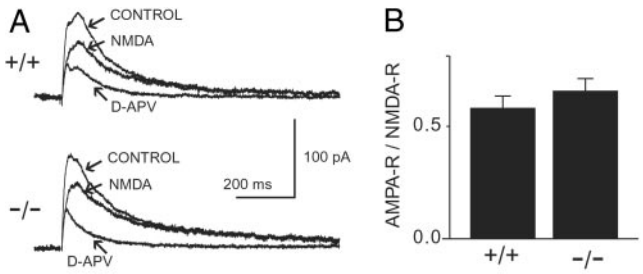

Fig. 6. Ratio of AMPA receptor (AMPA-R) to NMDA receptor (NMDA-R)-mediated synaptic responses in wild-type and Mint 1 knockout brains. (*A*) Representative averaged traces of EPSCs. Responses were recorded at a holding potential of +40 mV under control conditions or in the presence of 0.1 mM D-APV to measure AMPA-R responses (D-APV). The third trace (NMDA) displays the digital subtraction of the two experimental traces. (*B*) Summary ratio of AMPA-R- to NMDA-R-mediated synaptic responses (means ± SEMs; n = 10 cells from three wild-type and knockout mice).

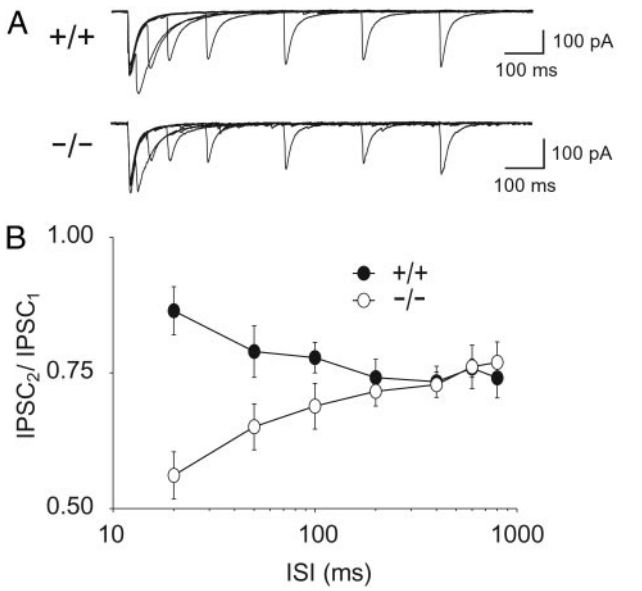

Fig. 7. Effect of Mint 1 knockout on inhibitory synaptic transmission. (*A*) Representative IPSCs elicited by paired-pulse stimuli delivered at different interstimulus intervals (ISIs) for wild-type (+/+) and knockout (−/−) mice averaged from 15 consecutive responses. (*B*) Paired-pulse depression at inhibitory synapses (means ± SEM) plotted as a function of the interstimulus interval for wild-type (n = 10 cells, four mice) and knockout (n = 10 cells, four mice) mice.

Based on an *in vitro* complex formed by the Mint 1–CASK heterodimer with the NMDA receptor and the motor protein Kif17, it was reported that the Mint 1–CASK heterodimer functions to transport NMDA receptors selectively to synapses (20). Because only Mint 1 binds to CASK, this function could not be redundant among Mints. Our data suggest that it is unlikely that Mint 1 is required for the synaptic delivery of NMDA receptors, because LTP is induced normally in the Mint 1 knockout mice (Fig. 5*D*). However, a partial impairment of NMDA-receptor function may have been overlooked in the LTP experiments because of the strong induction protocol used. Therefore we quantified the relative contributions of AMPA and NMDA receptors to the overall synaptic responses in hippocampal CA1 pyramidal cells by recording EPSCs at +40 mV before and after application of D-APV (Fig. 6*A*). The ratio of AMPA receptor- to NMDA receptor-mediated EPSCs was not affected in the Mint 1 knockout, effectively ruling out a mandatory role for Mint 1 in the trafficking of NMDA receptors to synapses.

Finally, we examined inhibitory synaptic transmission by recording monosynaptic IPSCs from CA1 pyramidal cells in response to paired-pulse stimulation. Under our recording conditions, IPSCs exhibit paired-pulse depression, which provides a sensitive measure of changes in the regulation of GABA release (35). We observed a large increase in paired-pulse depression at short interstimulus intervals (<100 ms; Fig. 7). This result suggests that deletion of Mint 1 causes a dramatic change in the regulation of GABA release, possibly by increasing the release probability, because this is the most common cause for enhanced paired-pulse depression.

Discussion

Our results suggest several unanticipated conclusions about the function of Mint 1. First, they indicate that the Mint 1–CASK complex does not perform an essential developmental function in mice, in contrast to *C. elegans* where the orthologous Lin-2–Lin-10 complex is essential for proper cell specification in vulval development (22). This conclusion is supported by an indepen-

dently reported Mint 1 knockout (41) that, although not analyzed beyond measurements of the response of mutant mice to methamphetamine, also exhibited no developmental abnormalities. Because only Mint 1 but not Mints 2 and 3 binds to CASK (Fig. 1), the apparent lack of a major function of the Mint 1–CASK complex in mice cannot be explained by redundancy among Mints.

Second, again in contrast to *C. elegans* where Lin-10 has a separate function in the targeting of AMPA-type glutamate receptors (23), we show that Mint 1 is not required for AMPA-receptor localization or function in mice. Because the *C. elegans* phenotype is CASK-independent, it is possible that in this respect Mints 2 and/or 3 are redundant with Mint 1; thus our data do not exclude a redundant role for Mints in AMPA-receptor trafficking.

Third, we also tested the prediction based on GST pull-down assays that Mint 1 is involved in transporting NMDA receptors to synapses by binding to CASK and Kif17 (20). Our data demonstrate that deletion of Mint 1 has no significant effect on NMDA receptor-mediated synaptic currents. Because the presumptive NMDA-receptor targeting function of Mint 1 depends on CASK, our data suggest that these *in vitro* binding data (20) do not reflect a physiological interaction.

Finally, our most important finding probably is that Mint 1 is essential for regulating inhibitory synaptic transmission. We observed a large change in paired-pulse depression in GABAergic synapses, suggesting that neurotransmitter release is altered. The direction of the change indicates that the deletion of Mint 1 may have increased the release probability at inhibitory synapses. Consistent with the discrete phenotype of Mint 1 knockout mice in inhibitory synapses, we found that in inhibitory interneurons, Mint 1 is selectively enriched over Mint 2, whereas excitatory neurons appear to express both Mints similarly. Thus the selective phenotype of the Mint 1 knockout mice in inhibitory neurons could be accounted for by the hypothesis that Mints 1 and 2 are fully functionally redundant in excitatory neurons but only partially redundant in inhibitory neurons. According to this hypothesis, Mints 1 and 2 (and possibly Mint 3) perform common synaptic functions by interactions with Munc18-1, APP, and/or Ca^{2+} channels. Alternatively, it is possible that the Mint 1–CASK complex performs a restricted function only in regulating release of GABA. Future experiments with double Mint 1/2 knockout mice will be required to test these hypotheses.

It is puzzling that the Mint 1 deletion causes a discrete synaptic phenotype even though the protein is enriched in the cell body and is present throughout the dendrites and axons without a specifically synaptic localization. This result suggests that either the nonsynaptic majority of Mint 1 protein in neurons is functionally irrelevant (which seems rather improbable) or that the synaptic effect of the Mint 1 deletion is an indirect consequence of a functional impairment outside of the synapse. It is possible, for example, that Mints normally function in the assembly of synapses from precursor vesicles that are generated in the trans-Golgi complex, possibly by binding to APP. Impairment of this function then could lead to a change in synaptic transmission, which would explain the phenotype observed here. Again, future experiments will have to address these ideas.

We thank I. Kornblum, A. Roth, and E. Borowicz for excellent technical assistance and N. Hamlin and A. Mercado for animal care. This study was supported by National Institutes of Health Grant R37-MH52804-06 (to T.C.S.) and National Institutes of Health Fellowship F32-AG05844 (to A.H.).

1. Duclos, F. & Koenig, M. (1995) *Mamm. Genome* **6,** 57–58.
2. Okamoto, M. & Südhof, T. C. (1997) *J. Biol. Chem.* **272,** 31459–31464.
3. Okamoto, M. & Südhof, T. C. (1998) *Eur. J. Cell Biol.* **77,** 161–165.
4. Tanahashi, H. & Tabira, T. (1999) *NeuroReport* **10,** 2575–2578.
5. Lau, K. F., McLoughlin, D. M., Standen, C. & Miller, C. C. (2000) *Mol. Cell. Neurosci.* **16,** 557–565.
6. Butz, S., Okamoto, M. & Südhof, T. C. (1998) *Cell* **94,** 773–782.
7. Borg, J. P., Straight, S. W., Kaech, S. M., de Taddeo-Borg, M., Kroon, D. E., Karnak, D., Turner, R. S., Kim, S. K. & Margolis, B. (1998) *J. Biol. Chem.* **273,** 31633–31636.
8. Borg, J. P., Lopez-Figueroa, M. O., de Taddeo-Borg, M., Kroon, D. E., Turner, R. S., Watson, S. J. & Margolis, B. (1999) *J. Neurosci.* **19,** 1307–1316.
9. Hata, Y., Butz, S. & Südhof, T. C. (1996) *J. Neurosci.* **16,** 2488–2494.
10. Hsueh, Y. P. & Sheng, M. (1999) *J. Neurosci.* **19,** 7415–7425.
11. Biederer, T. & Südhof, T. C. (2000) *J. Biol. Chem.* **275,** 39803–39806.
12. Biederer, T. & Südhof, T. C. (2001) *J. Biol. Chem.* **276,** 47869–47876.
13. Biederer, T., Cao, X., Südhof, T. C. & Liu, X. (2002) *J. Neurosci.* **22,** 7340–7351.
14. Biederer, T., Sara, Y., Mozhayeva, M., Atasoy, D., Liu, X., Kavalali, E. T. & Südhof, T. C. (2002) *Science* **297,** 1525–1531.
15. Verhage, M., Maia, A. S., Plomp, J. J., Brussaard, A. B., Heeroma, J. H., Vermeer, H., Toonen, R. F., Hammer, R., van den Berg, T. K., Missler, M., *et al.* (2000) *Science* **287,** 864–869.
16. Borg, J. P., Ooi, J., Levy, E. & Margolis, B. (1996) *Mol. Cell. Biol.* **16,** 6229–6241.
17. McLoughlin, D. M. & Miller, C. C. (1996) *FEBS Lett.* **397,** 197–200.
18. Zhang, Z., Lee, C. H., Mandiyan, V., Borg, J. P., Margolis, B., Schlessinger, J. & Kuriyan, J. (1997) *EMBO J.* **16,** 6141–6150.
19. Maximov, A., Südhof, T. C. & Bezprozvanny, I. (1999) *J. Biol. Chem.* **274,** 24453–24456.
20. Setou, M., Nakagawa, T., Seog, D. H. & Hirokawa, N. (2000) *Science* **288,** 1796–1802.
21. Whitfield, C. W., Benard, C., Barnes, T., Hekimi, S. & Kim, S. K. (1999) *Mol. Biol. Cell* **10,** 2087–2100.
22. Kaech, S. M., Whitfield, C. W. & Kim, S. K. (1998) *Cell* **94,** 761–771.
23. Rongo, C., Whitfield, C. W., Rodal, A., Kim, S. K. & Kaplan, J. M. (1998) *Cell* **94,** 751–759.
24. Jo, K., Derin, R., Li, M. & Bredt, D. S. (1999) *J. Neurosci.* **19,** 4189–4199.
25. Simske, J. S., Kaech, S. M., Harp, S. A. & Kim, S. K. (1996) *Cell* **85,** 195–204.
26. Kamal, A., Almenar-Queralt, A., LeBlanc, J. F., Roberts, E. A. & Goldstein, L. S. (2001) *Nature* **414,** 643–648.
27. Sastre, M., Turner, R. S. & Levy, E. (1998) *J. Biol. Chem.* **273,** 22351–22357.
28. Borg, J. P., Yang, Y., De Taddeo-Borg, M., Margolis, B. & Turner, R. S. (1998) *J. Biol. Chem.* **273,** 14761–14766.
29. Mueller, H. T., Borg, J. P., Margolis, B. & Turner, R. S. (2000) *J. Biol. Chem.* **275,** 39302–39306.
30. Ho, C. S., Marinescu, V., Steinhilb, M. L., Gaut, J. R., Turner, R. S. & Stuenkel, E. L. (2002) *J. Biol. Chem.* **277,** 27021–27028.
31. Zambrano, N., Bimonte, M., Arbucci, S., Gianni, D., Russo, T. & Bazzicalupo, P. (2002) *J. Cell Sci.* **115,** 1411–1422.
32. Rosahl, T. W., Spillage, D., Missler, M., Hers, J., Selig, D., Wolff, J. R., Hammer, R. E., Malenka, R. C. & Südhof, T. C. (1995) *Nature* **375,** 488–493.
33. Nagy, A., Rossant, J., Nagy, R., Abramow-Newerly, W. & Roder, J. C. (1993) *Proc. Natl. Acad. Sci. USA* **90,** 8424–8428.
34. O'Gorman, S., Dagenais, N. A., Qian, M. & Marchuk, Y. (1997) *Proc. Natl. Acad. Sci. USA* **94,** 14602–14607.
35. Schoch, S., Castillo, P. E., Jo, T., Mukherjee, K., Geppert, M., Wang, Y., Schmitz, F., Malenka, R. C. & Südhof, T. C. (2002) *Nature* **415,** 321–326.
36. Morishita, W., Connor, J. H., Xia, H., Quinlan, E. M., Shenolikar, S. & Malenka, R. C. (2001) *Neuron* **32,** 1133–1148.
37. Laemmli, U. K. (1970) *Nature* **277,** 680–685.
38. Towbin, H., Staehelin, T. & Gordon, J. (1979) *Proc. Natl. Acad. Sci. USA* **76,** 4350–4354.
39. Okamoto, M., Matsuyama, T. & Sugita, M. (2000) *Eur. J. Neurosci.* **12,** 3067–3072.
40. Maximov, A. & Bezprozvanny, I. (2002) *J. Neurosci.* **22,** 6939–6952.
41. Mori, A., Okuyama, K., Horie, M., Taniguchi, Y., Wadatsu, T., Nishino, N., Shimada, Y., Miyazawa, N., Takeda, S., Niimi, M., *et al.* (2002) *Neurosci. Res.* **43,** 251–257.